Predicting Operating Windows for High-Frequency Induction Aluminum Tube Welding

Machine learning was applied to predict viable operating windows for high-frequency induction welding of aluminum tubes for radiators

BY S.-W. CHENG AND H. ZHANG

Abstract

High-frequency (HF) induction welding is a practical welding technique widely used in various industries. Although it is generally robust, HF induction welding of aluminum tubes is complicated by the very high line speed, which requires high and accurate power input, and, therefore, a small fluctuation or variation in power input could result in drastically different welds. This work is dedicated to analyzing the influence of welding parameters, line speed, power input, and other unknown random factors, such as those induced by weather or work shift, especially those induced by the change of aluminum stock and adjustment/maintenance of the induction welding coil. Through the machine learning process, statistical models defining the normal operating windows were developed based on experimental data. The operating windows, defined by the overheat-normal and normal-cold boundaries, are expressed in terms of probabilities of producing normal welds. These trained models can be used to make new predictions, i.e., new operating windows, by collecting a small sample (a very limited number of calibrating data points). This procedure was verified experimentally.

Keywords

- Induction Welding
- Machine Learning
- Operating Windows

https://doi.org/10.29391/2023.102.013

Introduction

Aluminum tube welding is an important industrial process, and a major application of this technique is manufacturing radiators for automotive vehicles and air conditioners. These tubes are usually exposed to high pressure, high temperature, and vibrational loading in service. Such stringent requirements impose a serious challenge to the joining process in aluminum tube making. Aluminum welding has been a challenge in general because of aluminum alloys' high electrical and thermal conductivity, low melting temperature, and high thermal expansion coefficient (Ref. 1). The aluminum sheets used for making tubes for radiators are usually very thin (< 1 mm) with a limited allowable joining area, and a lap joint is difficult to attain. In addition, the high throughput of tube welding and stringent pressure tightness requirements complicate the process. High-frequency (HF) induction welding, a forge welding process, is a proven suitable technique for thin aluminum tube welding, and it has been widely adopted in the industry. In induction welding, a HF electromagnetic field is generated in the workpieces through an induction coil. Under resistive heating and/or heating by the hysteresis and forging force, a bond is formed at the faying interface. As a relatively mature joining technique, HF induction welding finds its applications in a large number of industrial processes, mainly because of its high tolerance to workpiece irregularities and process parameter variations. In HF induction welding, the induced heat is concentrated in a small volume of metal near the contact interface, so the process can produce welds at very high welding speed and with high energy efficiency.

Compared to low-frequency welding or resistance welding, HF welding requires much lower electric current and less power, with a narrow heat-affected zone and no superfluous cast structures (Ref. 2). It can be applied to welding both conventional steels and advanced high-strength steels. For

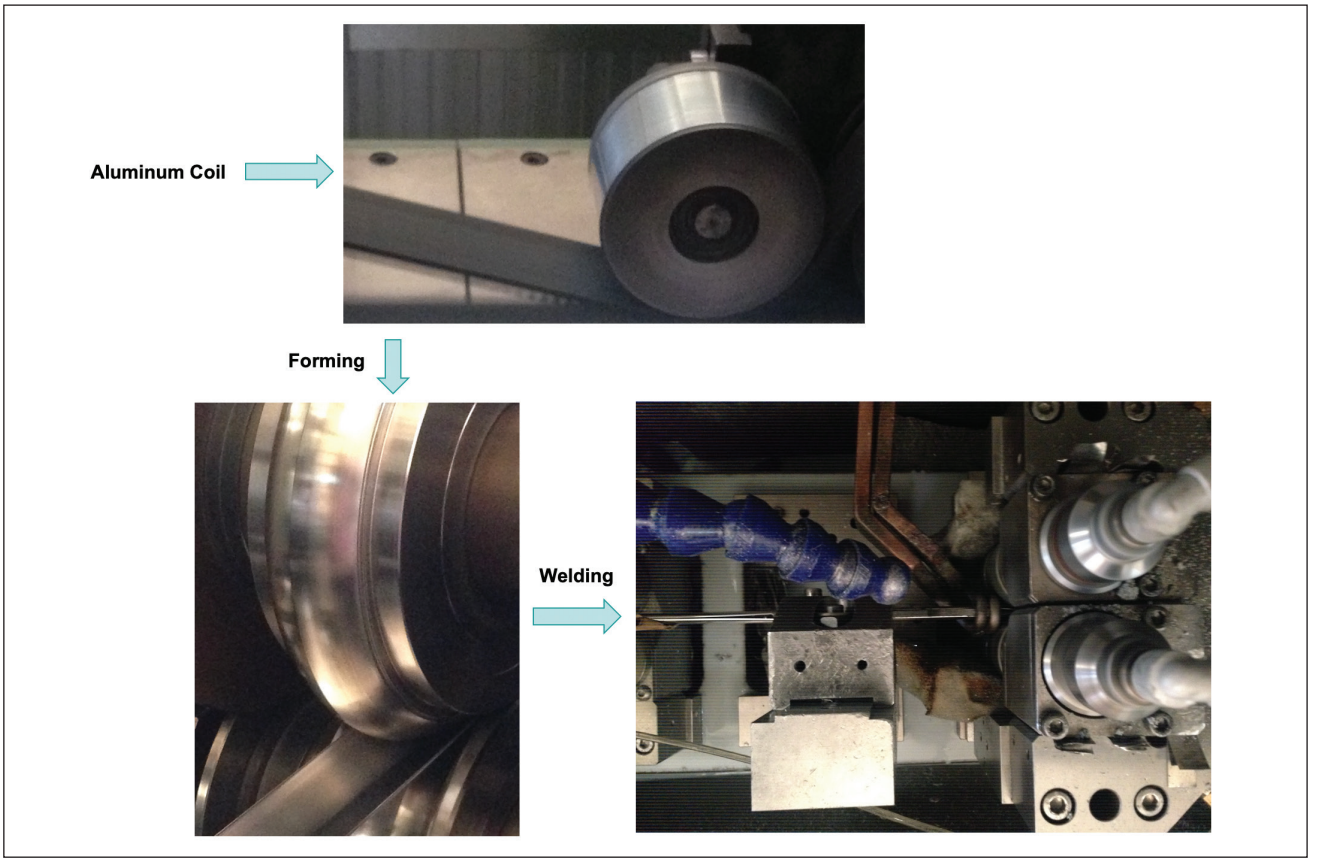

Fig. 1 — Major fabrication steps in aluminum tube making.

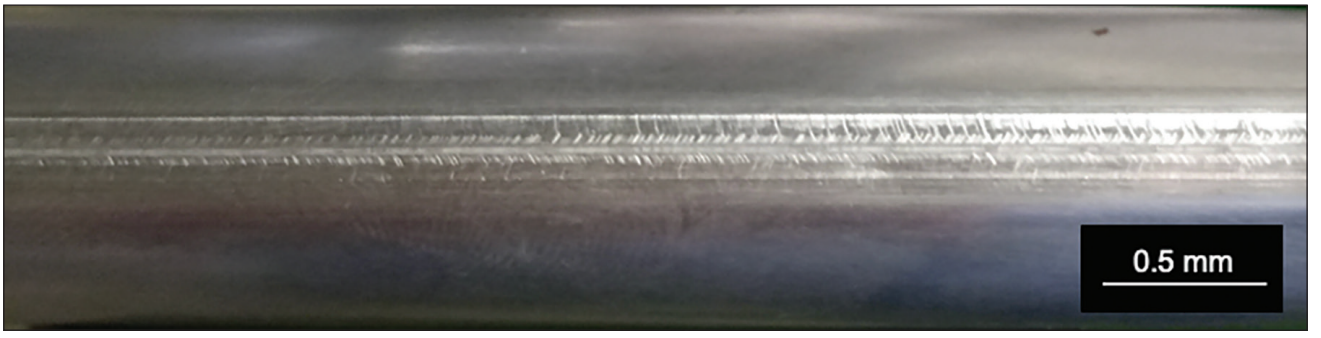

Fig. 2 — Weld joint of a HF induction-welded aluminum tube (top view).

instance, 2-mm- (0.08-in.) thick DP 780 and TRIP 780 steel sheets were successfully induction-welded to produce tubes of 76 mm (3 in.) in diameter for automotive applications (Ref. 3). Such tubes with butt-joint configuration could be fabricated without much difficulty, largely because steel welding is generally robust, and welding thick sheet is especially forgiving. However, HF welding of thin aluminum tubes is challenging in general; a small variance in the induction weld coil setup, or slight fluctuation in line speed or power input may drive the process out of the acceptance zone. Efforts have been made to improve the robustness of aluminum-thin tube manufacturing. For instance, induction brazing of aluminum tubes for solar collectors was studied through numerical and experimental studies, and an efficient induction brazing device was designed and optimal process parameters proposed (Ref. 4). Although the importance of controlling such a manufacturing process has been recognized by industrial practitioners, its process control algorithms are largely developed through trial and error, which is ineffective, time consuming, and costly. New approaches are called for in tackling this issue.

Machine learning (ML) is an effective means in dealing with complicated processes and has been applied to a number of manufacturing processes (Refs. 5–10). For instance, self-piercing riveting has been extensively studied through ML-assisted process simulation and control (Refs. 5–9). Multiple regression analysis and artificial neural network (ANN) models were used to predict the weld strength of copper-to-copper joints produced by ultrasonic welding, and it was found that ANN models predict more-accurate

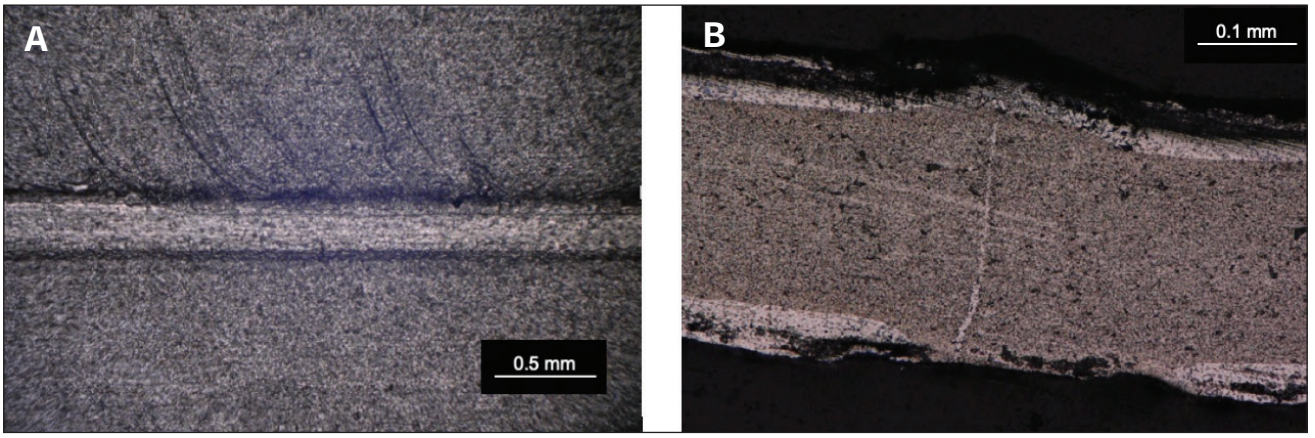

Fig. 3 — Specimens of a good weld. A — Top view; B — cross-sectional view of the joint's cross section.

results than conventional regression models (Ref. 10). Many welding processes have benefited significantly from adopting machine learning in-process control, as efficiency and accuracy have improved through intelligent welding quality monitoring and control (Ref. 11). In machine learning, unknown complicated processes have been treated largely as a black box, and new predictions are made through training and testing. Although this approach has been successful in dealing with many manufacturing processes, prediction accuracy may suffer if the training dataset is not large enough.

In this work, operating windows of aluminum tube welding were developed based on machine learning. Appropriate general statistical models were selected to represent the operating window's borders through training using experimental observations. The general operating windows were then specified for a particular welding setting using a small sample of experimental data obtained under that setting. This approach is not only necessary for HF induction welding of thin aluminum tubes, it also effectively avoids lengthy trial and adjustment and reduces scrap metals. The methodology developed in this process can also be applied to other applications in dealing with highly variable industrial processes.

High-Frequency Induction Aluminum Tube Welding

In HF induction welding of thin aluminum tubes, aluminum sheets are cut into narrow strips, formed through a series of rolls, and fed into the induction coil. The main steps are illustrated in Fig. 1. The aluminum strip is pulled in by the rolls at a fairly high speed, close to 100 m/min. The deformed aluminum strip goes through the induction coils, is heated by the induced electric current, and is joined along the butt-joint contact line. Experiments have shown that the welding parameters, power input, and line speed are somehow related. But such a relation is hard to attain, as there are many random effects that are difficult to account for, let alone to control. It was observed that speed, power, or both had to be adjusted when a new coil of aluminum strips was loaded, the squeeze roll position was adjusted, or when the production line was restarted after a normal termination between work shifts. A more-severe impact comes with normal maintenance of the induction coil, be it cleaning, adjustment, or part replacement. A historically proven set of process parameters can only serve as a guideline for selecting the line speed and power input. The conventional one-factor-at-a-time approach does not work well in this case, as the trials needed to develop a reasonable set of parameters can be numerous, and it is unrealistic to develop a complete operating window or an optimized welding schedule every time a change occurs.

The main quality requirement for these tubes was air tightness, which was tested through a pressure burst test. Figure 2 shows a section of aluminum tube made through the said induction welding process. Tubes of various cross-sectional shapes can be made through induction welding, and butt joints are usually used, as no special joint preparation is needed, and no material addition is necessary. However, the simple butt-joint configuration also poses a challenge to process stability. A small variation in fitup may create a root opening; slight underheating may produce a cold weld with insufficient joining strength; and slight overheating may render burn-through holes at the joint in addition to expulsion. In HF welding, material waste may result from poor fitup at the bonding interface and overheating in the form of expelled metal debris and burrs. Spattering during expulsion produces metal debris, which has to be removed, increasing production cost. Another consequence of overheating is distortion of the aluminum tubes produced, creating difficulties in assembly and resulting in leaking. These possible undesirable situations are complicated by variations in material and welding coil setup.

Specimens of aluminum tube welds made of AA3003/AA4045 clad sheets are presented in Figs. 3–5. Three types of welds were observed in production. A good weld, as seen in Fig. 3, has a clearly defined weld joint. A zoom-in of the weld joint shows scattering slagged metal debris on the weld joint but no burrs. The weld joint area is thickened due to induction heating and pressure exerted from the sides. The weld line is clear, fine, and uniform, indicating a quality joint. In contrast, when insufficient heat is supplied, the joining area is not sufficiently softened, leaving little or even no bonding — Fig. 4. The joint basically has no strength and no sealing capability. Although the heat is not enough to make a good joint, the amount of slags is visibly more than in a good weld.

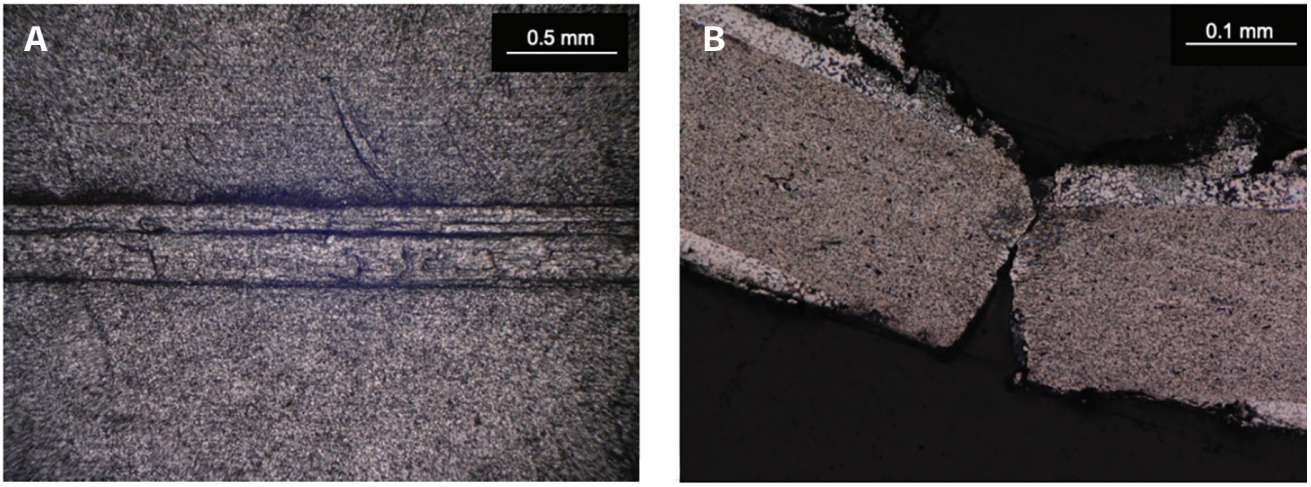

Fig. 4 — Specimens of a cold weld. A — Top view; B — cross-sectional view of the joint's cross section.

Table 1 — Commercial Compositions of AA3003 and AA4045 (wt-%) (Ref. 12)

Alloy	Si	Mn	Fe	Cu	Ti	Ni	Zn	Al
AA3003	0.219	1.066	0.553	0.073	0.006	0.008	0.003	Bal.
AA4045	9.857	0.004	0.156	0.001	0.012	0.007	0.001	Bal.

The insufficient heating leaves a continuous line inherited from the original surfaces at the butt joint. In an overheated joint, as seen in Fig. 5, much of the metal is wasted as slags and burrs. The thick burning marks on the weld joint surface are the evidence of too much heat supplied. In addition, there are also longitudinal as well as transverse cracks on the surface of the weld joint, possibly due to the loss of expelled metal, and shrinkage during cooling. The bond line, seen from the cross section, contains a long crack that originates from the root opening at the butt joint, providing minimal joining strength. In general, the quality of a tube weld can be easily judged by its appearance, and visual inspection is commonly employed in welding parameter selection and welding machine setup. From these figures, it can be seen that the amount of heat input must be accurately controlled in order to create a quality weld.

Experiment

The experiments for training, calibrating, and testing of ML models were conducted at an industrial company's production facility using the same type of aluminum sheets purchased from the same vendor over a period of one and a half years. 0.26-mm (0.01 in.) commercial sheets of AA3003 clad with AA4045 were used in production and the experiment. The commercial chemical compositions of this material are shown in Table 1. This ALCAD material is commonly used for products such as radiators because of its excellent high-temperature performance and corrosion resistance. In the experiment, line speed was varied between 70 and 90 m/min, and power input (kW) was varied in accordance to create a range of welds from cold to good/normal, and then to overheat welds. The level settings of welding schedules used in the experiment are presented in Figs. 6 and 7. Five repetitions were made for each welding schedule in the experiment.

Adjusting welding parameters is necessary every time a seemingly minor adjustment is made to the production line. The current practice is selecting the line speed and welding power through trial-and-error on the production line. A number of trials have to be made, regardless of the practitioner's experience, although they have a huge impact on the time spent to find a suitable welding schedule. An important characteristic of aluminum tube welding is that the outcomes are fairly consistent once welding parameters are set for a particular welding coil setup in a particular job shift. Results of all the repetitions (five of them) made successively due to the constraint of production conditions were identical. Therefore, no information on variation or random error could

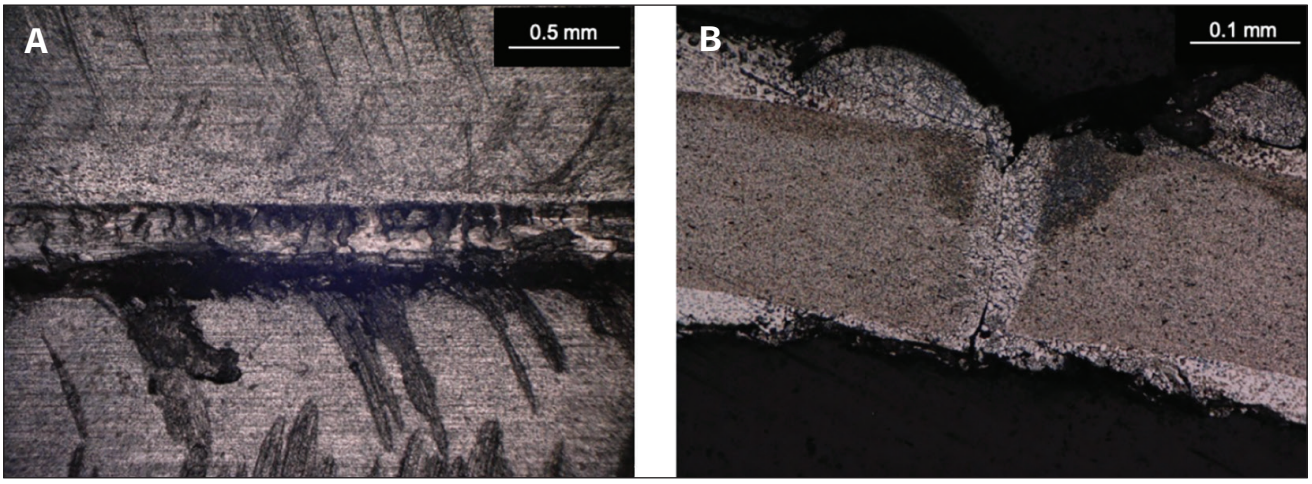

Fig. 5 — Specimens of an overheated weld. A — Top view; B — cross-sectional view of the joint's cross section.

Table 2 — Analysis of Deviance Results

Model	Residual DF	Residual Dev.	DF	Deviance	*p*-value
M_1	338	85.7072	6	286.6288	5.9835e–59
M_2	336	33.3776	2	52.3295	4.3330e–12
M_3	330	27.4642	6	5.9135	0.4329

be obtained in the experiment. However, certain variation was observed between welding schedules.

Machine Learning Analysis, Results, and Discussion

In production, feasible welding schedules (parameters) were developed through experimental trials. Such a process is time-consuming and costly, and the developed welding schedules may not be optimal. In addition, it only produces a single welding schedule that may lie near the border of an operating window, and a small disturbance in operation conditions, such as line power fluctuation, may push welding out of the acceptance range, resulting in inferior welds. The significant effects caused by the largely uncontrollable variables require the use of the machine learning concept in developing optimal operating windows in HF induction welding of thin Al tubes. The machine learning approach employed in this study involved data collection, statistical model development, verification, and new operating window predictions.

Data

Six sets of structured data were collected in the span of more than one year. Numerous tooling changes/adjustments and daily changes of aluminum coils were made during this period. Although these six sets were obtained at different periods, the first three sets of experiments were conducted in the first two quarters of the year, the fourth and fifth sets were conducted in the last quarter of the first year, and the last set, set #6, was obtained one and a half years after the start of the experiment. Therefore, the data were grouped accordingly as G_1 (sets 1, 2, 3), G_2 (sets 4, 5), and G_3 (set 6), and the first two were used for training. Part of the last data set, G_3 was used for calibrating, and the rest of it was used for testing.

There were three types of distinctive outcomes in aluminum tube welding: cold weld, normal weld, and overheat weld. Each dataset contained all three types of welds, and they could be used either as a whole with all three types of welds together or separately using data points regrouped into two subsets: one contained cold and normal welds, and another contained normal and overheat welds.

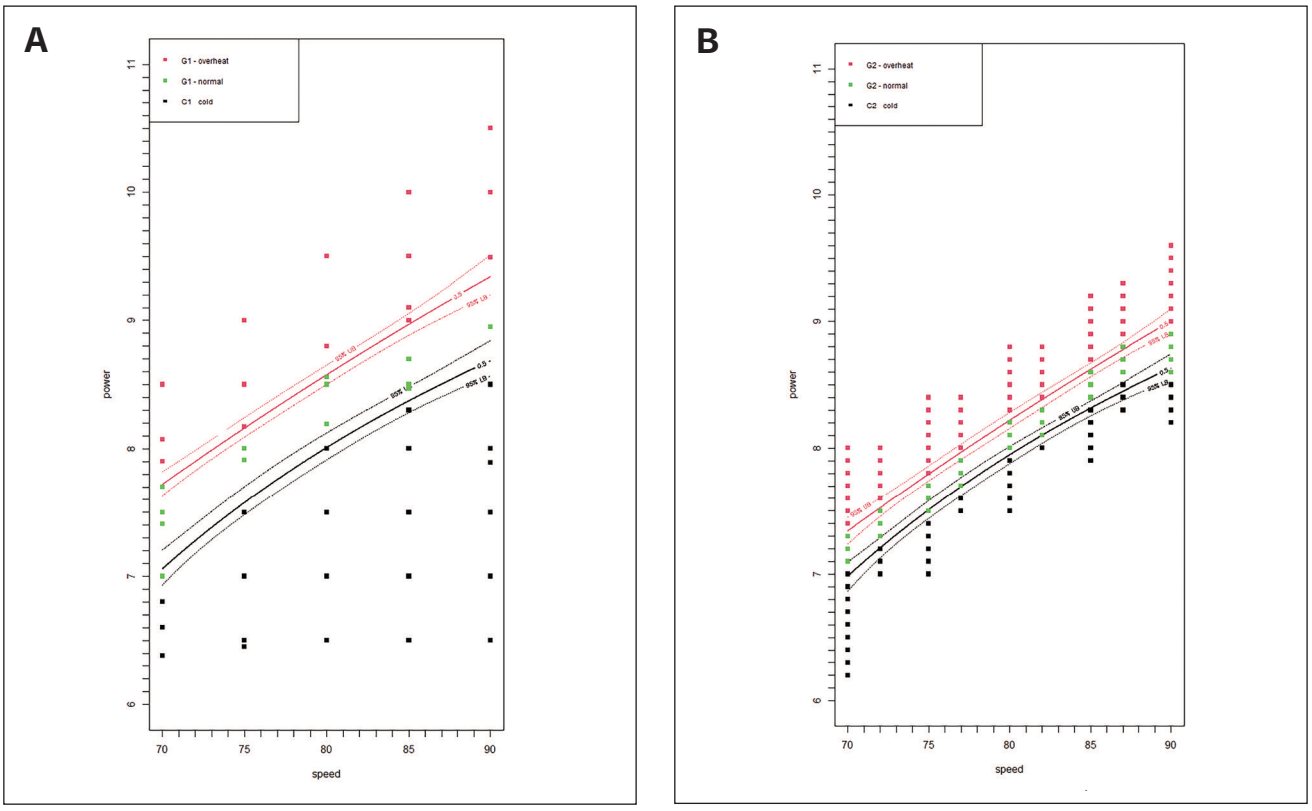

Fig. 6 — Probabilities of obtaining 50% normal welds created through training using G_1 (A) and G_2 (B).

Modeling

In production of thin aluminum tubes, the only controllable process parameters are *line speed* and *power*, and they can be digitally and accurately controlled. They were used as regular factors in the analysis. All other factors, known/unknown or controllable/uncontrollable, were lumped as an aggregated factor, known as *setting*. Factors and their values/levels used in the modeling are the following:

Line speed: 70 ~ 90 m/min

Power: Varied in accordance with *line speed* to produce cold, normal, and overheat welds

Setting: Lumped effect of induction welding coil adjustment/replacement, squeeze roll position, aluminum coil change, work shift, temperature, operator, and other unknown factors

Setting is very unique: It does not take any particular level or value, and it heavily affects weld quality. The working mechanisms of lumped variables, their influence, and even the number of such variables were largely unknown. Clearly, setting cannot be treated as a regular qualitative factor or a nuisance factor as its values/levels cannot be determined. Randomization does not help much, either, as its effect should be singled out, not averaged out. Therefore, it is hard to incorporate such a factor through conventional statistical analyses. Machine learning, on the other hand, has the advantages of dealing with situations such as this one, with complex and difficult-to-quantify influences, as it is able to detect patterns through experience derived from exposure to data.

Generalized first order models for multinomial responses (Ref. 13) with three categories (cold, normal, overheat) have proven to be appropriate for dealing with situations like aluminum tube welding with categorical data. The first step is to determine which factors and their interactions should be included in the statistical models. The following three models were evaluated on datasets G_1 and G_2.

M_1: response ~ *speed* + *power* + *speed* × *power*

M_2: response ~ *setting* + *speed* + *power* + *speed* × *power*

M_3: response ~ *setting* + *speed* + *power* + *speed* × *power* + (*speed* + *power* + *speed* × *power*): *setting*

The welding-related factors, *speed* and *power*, are often termed together as welding schedule and treated as quantitative variables, and *setting* was considered as a qualitative variable in the analysis.

Model M_1 assumes that *setting* has no effect. Model M_2 assumes that *setting* has a main effect but no interactions with other factors (i.e., it only causes the overheat-normal and normal-cold boundaries to shift up or down but does not change the shape of the boundaries). Model M_3 assumes that *setting* has a main effect and interactions with other factors. In M_3, the coefficients of *speed*, *power*, and *speed* × *power* may significantly change with *setting*. If M_3 is the appropriate model, the boundaries would be different in shape every time when *setting* changes. Note that M_1 is a sub-model of (or nested in) M_2, and M_2 is a sub-model of M_3.

If the experiment datasets supported M_1, there would be a fixed operating window and no adjustment would be needed as *setting* has no place in this model. However, the experi-

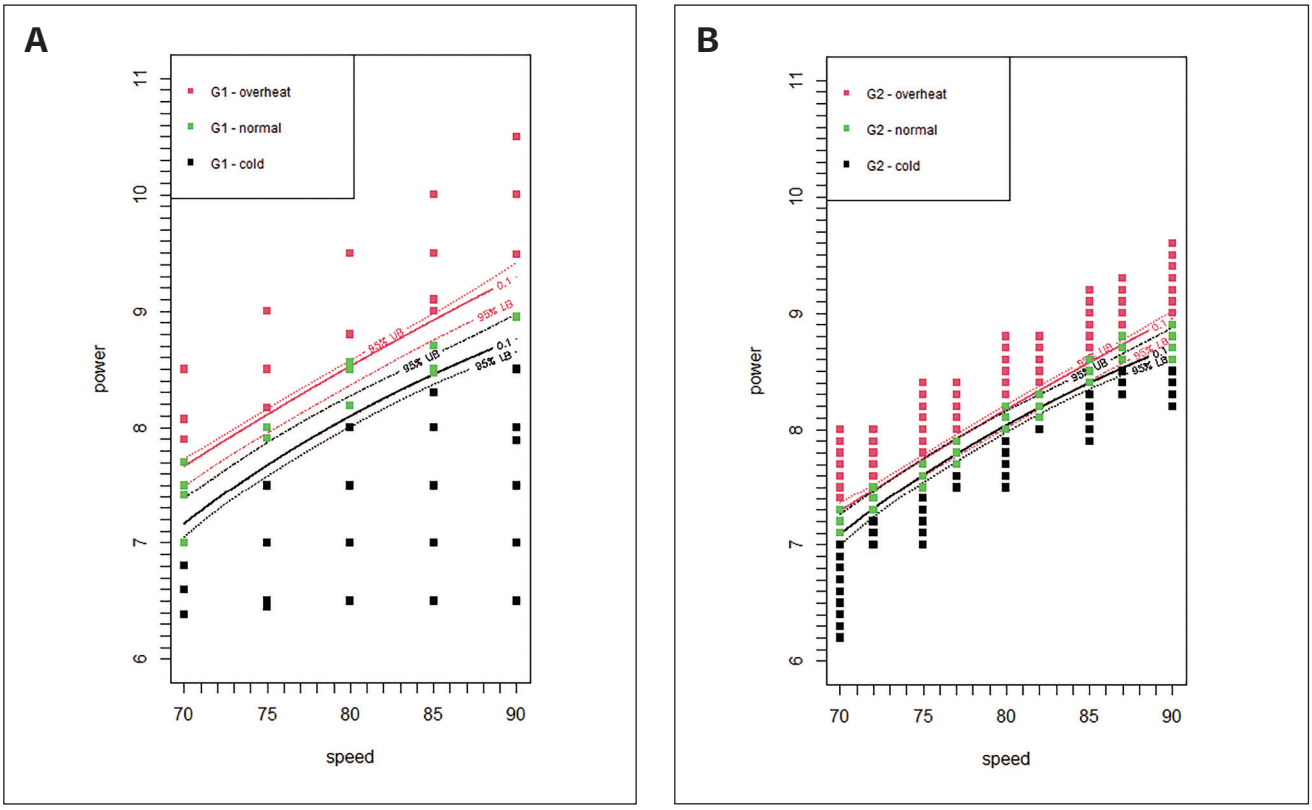

Fig. 7 — Probabilities of obtaining 90% normal welds created through training using G_1 (A) and G_2 (B).

mental observations clearly showed otherwise. If the data supported M_2, new data would only be needed at a specific *speed* in order to develop a new operating window by shifting the boundaries up or down, with their shapes unchanged. If the data supported M_3, new training data would have to be collected at multiple speeds (speed = 70, 75, 80, 85, 90 m/min for instance) in order to determine the shapes and locations of the new operating window boundaries. In other words, if M_3 was the appropriate model, all the previously collected data would have been useless in determining new operating windows and the model would have to be retrained every time when *setting* changes.

Model Selection

An analysis of deviance was conducted in order to evaluate the fits of these models and determine the most appropriate model among the three for the combined datasets of G_1 and G_2. The results are listed in Table 2.

A model with a small *p*-value indicates a good fitting of the model to the data. However, the appropriateness of a model should not be judged solely by its *p*-value; engineering sense plays a more-crucial role. Among the three models, M_1 had a very small *p*-value, yet it was not an appropriate model as it does not contain *setting*. Its extremely small *p*-value showed that speed and power are crucial in interpreting the categorical response, which is of no surprise. M_2 is the best among these three models, not only because its *p*-value was very small but because it reflected the influence of all factors involved. Compared to M_2, the more sophisticated model M_3 did not improve the fit at all, and the simpler model M_2 was preferred. M_2 appears to be the most appropriate for the combined dataset and would be used for modeling the responses; i.e., the probabilities of getting certain outputs (cold welds, normal welds, and overheat welds).

Training

Using datasets G_1 and G_2, model M_2 was fitted to estimate the probabilities of getting three categories of welds in induction welding of aluminum tubes. The estimated probabilities are denoted by $\hat{p}_0$ for cold welds, $\hat{p}_1$ for normal welds, and $\hat{p}_2$ for overheat welds, respectively, where $\hat{p}_0 + \hat{p}_1 + \hat{p}_2 = 1$. They are linked with the fitted coefficients of the generalized first order models by

$$\hat{p}_0 = \frac{\exp(\hat{\eta}_0)}{1+\exp(\hat{\eta}_0)}, \qquad \hat{p}_2 = \frac{\exp(\hat{\eta}_2)}{1+\exp(\hat{\eta}_2)}, \qquad \hat{p}_1 = 1 - \hat{p}_0 - \hat{p}_2 \quad (1)$$

where $\hat{\eta}_0$ and $\hat{\eta}_2$ are coefficients of the probabilities, representing the selected model (i.e., model M_2) for the relationship among the process parameters. The logistic models were trained using both the whole dataset and subsets of G_1 and G_2. It was observed that for both G_1 and G_2, the models developed (i.e., $\hat{\eta}_0$ and $\hat{\eta}_2$ derived) using these two data sets were effectively identical and, therefore, only one of the datasets was needed. The fitted logistic models

for $\hat{p}_0$ and $\hat{p}_2$, derived separately using the subsets of each data set, are presented here.

For dataset G_1, the fitted coefficients were

$$\begin{aligned}\hat{\eta}_0 &= -222.509 + 5.229\ speed + 8.484\ power - 0.412\ speed \cdot power \\ \hat{\eta}_2 &= 80.256 - 5.857\ speed + 24.780\ power + 0.256\ speed \cdot power\end{aligned} \quad (2)$$

and for dataset G_2, the fitted coefficients were

$$\begin{aligned}\hat{\eta}_0 &= -224.005 + 5.229\ speed + 8.484\ power - 0.412\ speed \cdot power \\ \hat{\eta}_2 &= 96.392 - 5.857\ speed + 24.780\ power + 0.256\ speed \cdot power\end{aligned} \quad (3)$$

Note that in these fitted models, the coefficients of *speed*, *power*, and *speed* × *power* were the same even as the models were trained using different datasets; only the intercept terms were affected by the data used. Such an observation indicates that the probability distribution of normalized data and its dependence on speed and power do not change for both the cold-normal and normal-overheat boundaries. In terms of operating windows, this means that the shape of an operating window does not change; only its location and width change with the data used. An operating window's location and width are determined by the intercepts in $\hat{\eta}_0$ and $\hat{\eta}_2$, which can be derived using a small number of data points. Therefore, it is possible to predict an operating window in terms of its boundaries between normal and inferior welds when any changes in setting, such as aluminum coil change, induction welding coil adjustment, etc., are made using very few data points.

Figures 6 and 7 present the operating windows drawn using the models derived from fitting using datasets G_1 and G_2. The borders of the operating windows were drawn as the probabilities of getting 50% normal welds with the upper and lower boundaries corresponding to ($\hat{p}_0$, $\hat{p}_1$, $\hat{p}_2$) = (0.0, 0.5, 0.5) and ($\hat{p}_0$, $\hat{p}_1$, $\hat{p}_2$) = (0.5, 0.5, 0.0) (Fig. 6), and to ($\hat{p}_0$, $\hat{p}_1$, $\hat{p}_2$) = (0.0, 0.9, 0.1) and ($\hat{p}_0$, $\hat{p}_1$, $\hat{p}_2$) = (0.1, 0.9, 0.0) (Fig. 7). The figures also show the 95% confidence intervals of the borders. A few observations can be made through examining these two figures:

1. The statistical boundaries were consistent with the shapes revealed by the data, indicating a good fit of the models to the training data.

2. Although the two operating windows created using G_1 and G_2 had different sizes (widths) and were placed at different locations, their borders were of exactly the same shape, consistent with the observations made from Equations 2 and 3.

3. It is also worth noting that the operating windows derived from G_1 and G_2 had no overlap, meaning that past experience, although rendering important shape information, is of little help for determining the location and width of a new operating window. Therefore, a new operating window has to be derived every time the setting changes, with borders of the same shape, but location/width derived using new data.

4. The 50% normal weld operating windows shown in Fig. 6 were wider than those of 90% normal welds in Fig. 7, as one would expect. This is due to the fact that making a good weld with high confidence requires tighter or more-precise control. From a practical point of view, a 90% normal weld window is preferable to a 50% normal weld window, as it provides higher confidence of producing quality welds. In addition, the windows produced through training dataset G_2 were much narrower than those using G_1 for both 50% and 90% normal welds. In general, a wide operating window is preferred, as a narrow or tight operating window leaves little room for process fluctuation.

5. The borders of the operating windows, although not completely linear, were fairly straight, as seen in all the figures. As the power input and line speed together determine the energy input rate, this observation indicates that the rate of energy input, or heating rate, should be kept roughly constant in order to produce a reasonable weld. As the heating rate is proportional to the power input and dwell time and the latter is inversely proportional to line speed, the heating rate can be approximately expressed as

$$heating\ rate \propto \frac{power}{line\ speed} \quad (4)$$

Therefore, the boundaries in an operating window can be produced once the maximum heating rate and minimum heating rate, corresponding to normal-overheat and normal-cold boundaries, respectively, are determined. The difference in locations of operating windows created using different datasets can be understood as the result of variation in heating conditions caused by changes in setting.

Calibration and Prediction

As the statistical models for the operating windows were proven adequate, they were used for predicting new operating windows. Using a dataset obtained with a new level of setting, such as G_3, the fitted models under M_2 would have the same coefficients as those with other setting levels except the intercepts. Unlike in many machine learning applications where new predictions are generally produced by trained models using training datasets, the trained models using G_1 and G_2 contain undetermined parameters, the intercepts of $\hat{\eta}_0$ and $\hat{\eta}_2$, when the prediction is made on a new setting. Conducting a new experiment and collecting a new set of data are required to estimate the intercepts to reflect the changes in operating conditions. This procedure is referred to as calibration.

The new intercepts can be estimated using very few data points. It is, therefore, proposed to make observations at one particular line speed and various power input values. This was demonstrated through a calibration using those points of G_3 with *speed* = 80, which are shown in Fig. 8A and called G_3S80 data, as the calibrating data, pretending that G_3S80 data was collected alone for predicting the operating window. Note that this calibrating dataset contains much fewer data points than G_1 or G_2. The new intercepts were estimated by fitting model M_2 using dataset G_3S80. In the new fit of M_2, the estimated coefficients are

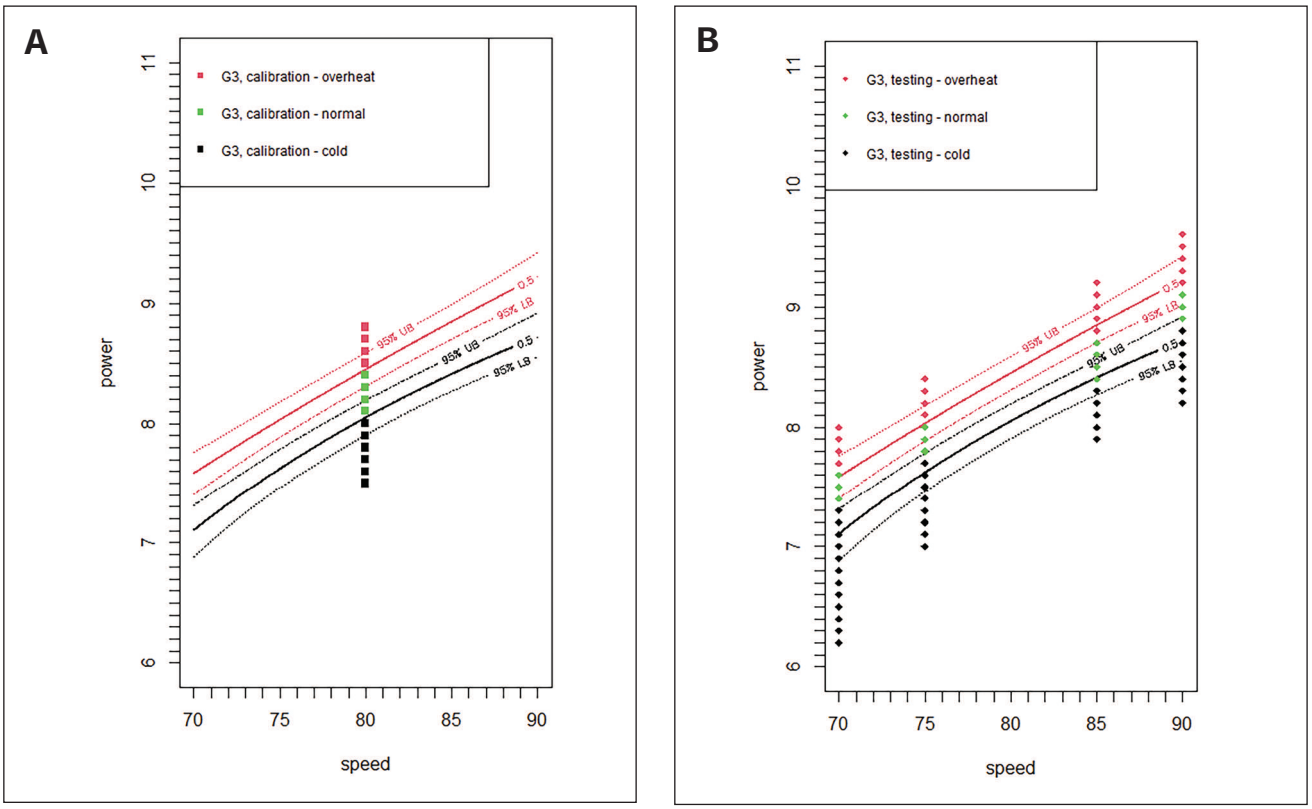

Fig. 8 — A — Predicted operating window derived using calibration data at speed = *80; B — a graphical comparison of the predicted operating window with the testing data. The probabilities of getting normal welds are 0.50.*

$$\hat{\eta}_0 = -221.509 + 5.229\ speed + 8.484\ power - 0.412\ speed \cdot power$$
$$\hat{\eta}_2 = 86.827 - 5.857\ speed + 24.780\ power + 0.256\ speed \cdot power \quad (5)$$

The intercepts derived are -222.509, -224.005, and -221.509 for $\hat{\eta}_0$, and 80.256, 96.392, and 86.827 for $\hat{\eta}_2$, using G_1, G_2, and G_3S80, respectively. The difference in intercepts reflects the difference in the locations of the operating windows. When fitting models for the intercepts using G_3S80, the same shape-related coefficients as in Equations 2 and 3 were used, assuming that the boundary shapes did not change. The assumption that the shapes of the operating window's borders remain the same for all settings, as observed in Equations 2 and 3 when fitting using G_1 and G_2, was further verified by a trial using the entirety of dataset G_3 for estimating all the coefficients of $\hat{\eta}_0$ and $\hat{\eta}_2$. The coefficients determined in this trial are extremely close to, although not exactly the same as, those in Equation 5. Therefore, the operating windows can be assumed to have the same shape, and only their location and width may vary with setting.

Testing

Figure 8B plots the data points of G_3 at speeds other than 80 m/min, which are regarded as testing data, together with the predicted operating window of 50% normal welds developed using dataset G_3S80, and it shows a good match between the predicted operating window and experimental observations. At every speed, the splits between cold-normal welds or normal-overheat welds almost always fell in the 95% confidence intervals of the boundaries. Therefore, the accuracy of the predicted operating window of G_3 was validated and confirmed by the testing data. However, the boundaries in Fig. 8B do not perfectly split the testing data as observed in Figs. 6 and 7 for training datasets G_1 and G_2. The reason is that the testing dataset G_3 was not used in developing the boundaries in Fig. 8B; it was only used for a real-world check. An operating window of 90% normal welds was also produced using the same model, plotted in Fig. 9, with more accurate fitting to the testing data yet a narrower width compared to that shown in Fig. 8. The results in Figs. 8 and 9 demonstrate that the predicted operating window, or the whole procedure including training and calibrating, is useful and accurate in real-world applications.

The fact that the shapes of the boundaries of an operating window remain unchanged indicated that the underlining physical processes during welding (i.e., heating, melting, and solidification) did not change. Other factors, such as reloading aluminum stock and induction coil adjustment that are highly unpredictable/uncontrollable, have a more significant impact on the welding schedule as they affect the width and location of the operating windows. The operating windows are generally fairly narrow, and those of high accuracy, e.g., 90% normal welds, are narrower than those of lower accuracy. The narrow operating windows indicate high sensitivity of the welding process to power input. The drastically different locations and sizes of the operating windows seen in the

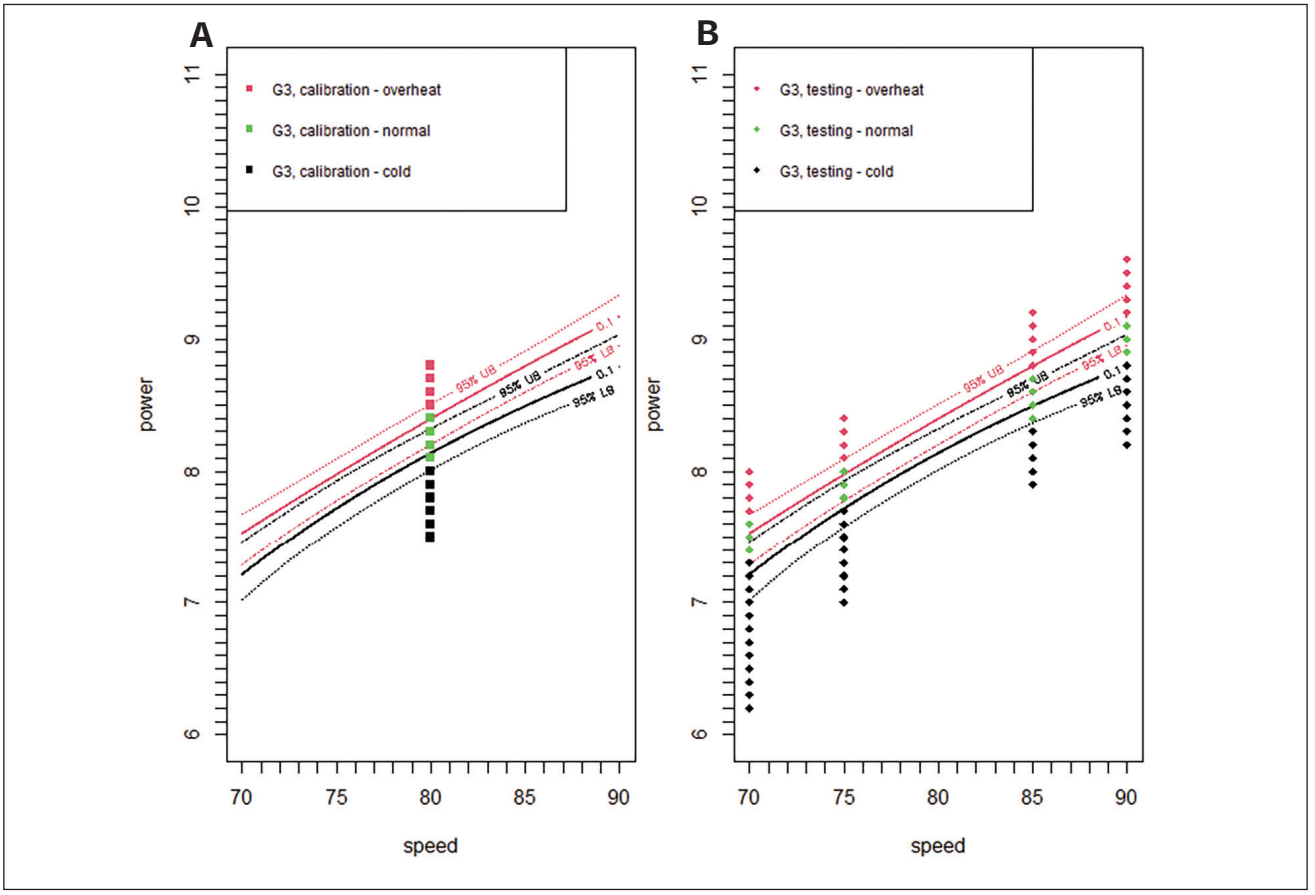

Fig. 9 — A — Predicted operating window derived using calibration data at speed = *80; B — a graphical comparison of the predicted operating window with the testing data. The probabilities of getting normal welds are 0.90.*

figures are clear evidence that this process should not be treated as a black box, and it is impossible to make reliable predictions without conducting new calibration tests.

Conclusions

In this research, machine learning was applied to predict viable operating windows for HF induction welding of aluminum tubes for radiators. Rapid yet accurate prediction of operating windows can be made through training and testing. The main findings are as follows:

1) In addition to the welding parameters, line speed, and power input, induction welding of aluminum tubes is also heavily affected by other factors, such as material and equipment maintenance. However, statistical analysis has shown that no significant interactions exist between these factors and welding parameters.

2) For induction welding of aluminum tubes, training data is helpful, as reflected in the unchanged shapes of the operating window borders produced through training. But a universal operating window is not attainable, no matter how large the training dataset. Prediction can only be made through training the models of general form using data generated in the new production environment.

3) As the boundaries in an operating window do not change shape when the production conditions change, predictions of new operating windows can be made by conducting a limited number of new tests for determining the locations of the boundaries.

4) Operating windows are the prediction results made through machine learning in this investigation, instead of individual points (welding schedules), as in many industrial applications of machine learning. This not only provides more choices for welding practitioners; it is also possible to gain a better understanding of the underlining physical processes through such analysis. This practice may expand the scope of machine learning applications.

5) Narrow operating windows indicate high sensitivity of the induction welding process to energy input, and extreme

caution should be taken when choosing welding parameters to avoid inferior welds.

This research addressed a distinct set of challenges that cannot be forecasted merely through model training; it necessitates conducting fresh experiments for accurate predictions. The methodology adopted in this research can be applied to other manufacturing processes that although governed by fundamental engineering principles, a seemingly minor but uncontrollable change may produce drastically different output. Past data alone, used as training data in machine learning, are helpful but may not produce valid predictions for certain processes, such as the one in this study.

Acknowledgment

The authors would like to express their appreciation for the financial support and technical assistance of XinHeYuan Inc. of Shandong Province, China.

References

1. Zhang, H., and Senkara, J. 2011. *Resistance Welding: Fundamentals and Applications*, 2nd Ed. CRC Press, Boca Raton, Fla.

2. HF Welding Parameters and Procedures. Retrieved October 16, 2022, from *ahssinsights.org/tag/induction-seam-welding-of-pipe-and-tubing/*.

3. Rashid, M., Martin, P., Biro, E., and Soldaat, R. 2010. Effect of chemistry on the heat-affected zone softening during induction welding of advanced high-strength steel tubes. *Proceedings of the Sheet Metal Welding Conference XIV*: Paper 2-3.

4. Demianová, K., Behúlová, M., Ožvold, M., Turňa, M., and Sahul, M. 2012. Brazing of aluminum tubes using induction heating. *Advanced Materials Research* 463-464 (2012): 1405–1409.

5. Fang, Y., Huang, L., Zhan, Z., Huang, S., Liu, X., Chen, Q., Zhao, H., and Han, W. 2022. A framework for calibration of self-piercing riveting process simulation model. *Journal of Manufacturing Processes* 76: 223–235.

6. Karathanasopoulos, N., Pandya, K. S., and Mohr, D. 2021. Self-piercing riveting process: Prediction of joint characteristics through finite element and neural network modeling. *Journal of Advanced Joining Process* 3(2): 100040.

7. Thomas, T., Markus, I., Martin-Friedrich, G., Klaus, D., and Klaus, D. 2018. Robust joining point design for semi-tubular self-piercing rivets. *The International Journal of Advanced Manufacturing Technology* 98: 431–440.

8. Oh, S., Kim, H. K., Jeong, T. E., Kam, D. H., and Ki, H. 2020. Deep-learning-based predictive architectures for self-piercing riveting process. *IEEE Access PP* (99): 1–1.

9. Lin, J., Qi, C., Wan, H., Min, J., Chen, J., Zhang, K., and Zhang, L. 2021. Prediction of cross-tension strength of self-piercing riveted joints using finite element simulation and XGBoost algorithm. *Chinese Journal of Mechanical Engineering* 34(1): 1–11.

10. Anand, K., Elangovan, S., and Rathinasuriyan, C. 2018. Modeling and prediction of weld strength in ultrasonic metal welding process using artificial neural network and multiple regression method. *Material Science & Engineering International Journal* 2(2): 39–46. DOI: 10.15406/mseij.2018.02.00032

11. Mahadevan, R., Jagan, A., Pavithran, L., Shrivastava, A., and Selvaraj, S. K. 2021. Intelligent welding by using machine learning techniques. *Materials Today: Proceedings, 3rd International Conference on Materials, Manufacturing and Modelling* 46(17): 7402–7410.

12. Caron, E., Ortega Pelayo, R., Baserinia, A., Wells, M., Weckman, D., Barker, S., and Gallerneault, M. 2014. Direct-chill co-casting of AA3003/AA4045 aluminum ingots via Fusion™ technology. *Metallurgical and Materials Transactions B* 45B: 975–987.

13. Agresti, A. 2013. *Categorical Data Analysis*, 3rd Ed. Chapter 8. Hoboken, N.J.: John Wiley & Sons Inc.

SHAO-WEI CHENG (*swcheng@stat.nthu.edu.tw*) is with the National Tsing Hua University, Taiwan, Republic of China. **HONGYAN ZHANG** is with The University of Toledo, Toledo, Ohio.